Pergamon

Geochimica et Cosmochimica Acta, Vol. 66, No. 7, pp. 1159–1169, 2002

0016-7037/02 $22.00 + .00

PII S0016-7037(01)00852-3

Comparison of two potential strategies of planktonic foraminifera for house building: Mg^{2+} or H^+ removal?

RICHARD E. ZEEBE[1,2,*] and ABHIJIT SANYAL[2]

[1]Alfred Wegener Institute for Polar and Marine Research, Am Handelshafen, D-27570, Bremerhaven, Germany
[2]Lamont-Doherty Earth Observatory of Columbia University, Route 9W, Palisades, New York 10964, USA

(*Received March* 15 2001; *accepted in revised form October* 31, 2001)

Abstract—Marine organisms must possess strategies enabling them to initiate calcite precipitation despite the unfavorable conditions for inorganic precipitation in surface seawater. These strategies are poorly understood. Here we compare two potential strategies of marine calcifyers to manipulate seawater chemistry in order to initiate calcite precipitation: Removal of Mg^{2+} and H^+ ions from seawater solutions. An experimental setup was used to monitor the onset of inorganic precipitation on seed crystals as a function of the Mg^{2+} concentration and *p*H in artificial seawater. We focused on precipitation rates typical for biogenic calcification in planktonic foraminifera ($\sim 10^{-3}$ mol m^{-2} h^{-1}) and time scales typical for the initiation of calcification in these organisms (minutes to hours). We find that the carbonate ion concentration has to increase by a factor of ~13 when $[Mg^{2+}]$ increases from 0 to 53 mmol kg^{-1} in order to maintain a typical biogenic precipitation rate. Model calculations for the energy requirement for various scenarios of Mg^{2+} and H^+ removal including Ca^{2+} exchange and CO_2 diffusion are presented. We conclude that the more cost-effective strategy to initiate calcite precipitation in foraminifera is H^+ removal, rather than Mg^{2+} removal. *Copyright © 2002 Elsevier Science Ltd*

1. INTRODUCTION

In the ocean, inorganic precipitation of calcium carbonate is rarely observed. Although surface seawater is about 4 and 6 times supersaturated with respect to aragonite and calcite, respectively, inorganic precipitation in the ocean is a scarce phenomenon, occurring only at a few locations such as in the Bahama Banks and the Persian Gulf. In order to explain the lack of extensive inorganic precipitation in the surface ocean, it has been suggested that the surfaces of potential precipitation nuclei are poisoned by various substances which inhibit nucleation and crystal growth of $CaCO_3$ in seawater. Among those substances are dissolved organic compounds, phosphate, and magnesium (e.g., Simkiss, 1964; Chave and Suess, 1970; Berner, 1975; Berner et al., 1978; Mucci and Morse, 1983; Mucci, 1986; Lebrón and Suárez, 1998; for summary, see Morse and Mackenzie, 1990).

The vast majority of marine calcium carbonate is produced by organisms which secrete calcitic or aragonitic skeletons. The major calcite producers in the open ocean are coccolithophorids and foraminifera, while the most abundant aragonite organisms are pteropods. The global annual production of pelagic calcium carbonate has recently been estimated as 58×10^{12} mol C y^{-1}, equivalent to approximately 0.7 Gt C y^{-1} (Milliman et al., 1999). Apparently, organisms are capable of producing large amounts of $CaCO_3$ despite the unfavorable conditions for inorganic precipitation in surface seawater. They must therefore possess certain strategies to overcome potential nucleation-inhibiting effects, enabling them to initiate $CaCO_3$ precipitation.

In this paper we focus on magnesium as an inhibitor of calcite precipitation. It is hypothesized that one potential strategy for shell formation of calcite secreting organisms such as planktonic foraminifera is the manipulation of the Mg^{2+} concentration at the site of calcification. This hypothesis is based mainly on two observations. First, magnesium has an inhibiting effect on calcite precipitation (e.g., Berner et al., 1975; Mucci and Morse, 1983; Zhang and Dawe, 2000; Davis et al., 2000). The removal of Mg^{2+} ions at the site of calcification would therefore greatly enhance the growth of the calcite crystal. Second, planktonic foraminifera produce low-magnesian calcite (~0.1–1 mol % $MgCO_3$, e.g., Nürnberg et al., 1996; Lea et al., 1999) compared to high-magnesian calcite precipitated inorganically from natural or artificial seawater (~6–25 mol % $MgCO_3$) and high-magnesian calcite of abiotic marine origin (~5–20 mol % $MgCO_3$, e.g., Mucci, 1987; Morse and Mackenzie, 1990; Carpenter and Lohmann, 1992). The latter observation suggests that planktonic foraminifera control the magnesium concentration in their calcite shells and might therefore manipulate the Mg^{2+} concentration of the calcifying fluid at the site of calcification.

As a first step towards a better understanding of the effect of magnesium on biogenic calcite precipitation, we consider a highly simplified calcification model. In the model, calcite is precipitated from a volume of seawater which is closed to ion exchange with the exception of Mg^{2+} and H^+ ions that are exchanged for other specific ions. Of course, the model is at best a crude approximation to a possible subprocess of biogenic calcification. Nevertheless, models of this kind can be very useful for understanding the inorganic basis of such processes (e.g., McConnaughey, 1989; Zeebe, 1999). The question to be asked is: At which magnesium concentration and *p*H will calcite start to precipitate at rates typical for biogenic calcification if precipitation nuclei are present? In order to address this question, we used an experimental setup and monitored the onset of inorganic precipitation on calcite seed crystals as a

* Author to whom correspondence should be addressed (Electronic mail: rzeebe@awi-bremerhaven.de).

function of the Mg^{2+} concentration and *p*H in artificial seawater. The model described here may correspond to a situation in which a calcifying organism, e.g., a planktonic foraminifer, manipulates a volume of seawater by removing Mg^{2+} or H^+ ions in order to initiate calcite precipitation.

We focus our study on planktonic foraminifera. The reason for this is that in order to compare our results from inorganic precipitation experiments to biogenic calcification, the calcifying organism considered has to meet certain criteria. The organism should be among the most important marine calcifying groups, the mineral deposited should be low-magnesian calcite, and the timing of the initiation of calcite precipitation and calcification rates should be known in some detail. This holds true for planktonic foraminifera. Corals and pteropods produce aragonite while benthic foraminifera also produce high-magnesian calcite. We could include coccolithophores in our discussion but much less is known about the timing of the initiation of calcite precipitation and calcification rates in their internal vesicles. In addition, Mg/Ca ratios in coccolithophores have not been studied in such detail as in foraminifera.

Foraminifera use an organic matrix for the initiation of calcite precipitation (e.g., Hemleben et al., 1977; Bé et al., 1979; Weiner and Erez, 1984). It is believed that the primary role of this matrix is to provide initial nucleation sites for the crystallization process (e.g., Lowenstam and Weiner, 1989; Simkiss and Wilbur, 1989). In order to mimic such an initial surface for nucleation in our experiments, we used seed crystals on which ordered growth of calcite occurred. This avoids, for instance, spontaneous crystallization on the walls of the vessel which would make the comparison with the situation in foraminifera more difficult.

The time scale and precipitation rate considered in our approach is crucial to the potential applicability of the simple model to the real situation. The time scale for the onset of chamber formation in planktonic foraminifera is on the order of minutes to hours (e.g., Hemleben et al., 1989). If removal of Mg^{2+} or H^+ ions is a strategy used by planktonic foraminifera to initiate calcite precipitation, this mechanism must therefore be capable of initiating crystal growth within minutes at proper precipitation rates. It is well known that the onset of calcite precipitation might take hours to days even if the solution is highly supersaturated (e.g., Morse et al., 1980). In other words, it is possible that after a sufficiently long time period calcite precipitates from a supersaturated solution in which initially no precipitation was observed. The investigation of this phenomenon is, however, not the subject of this paper because we are primarily interested in small time scales typical for the onset of biogenic calcification. The goal of this study is the determination of the critical supersaturation as a function of $[Mg^{2+}]$ and *p*H that is required to initiate calcite precipitation on seeds within minutes, and at precipitation rates similar to biogenic precipitation rates. We do not focus on the determination of equilibrium conditions, i.e., the solubility of calcite as a function of the magnesium concentration, which has been described elsewhere (e.g., Mucci and Morse, 1984).

2. EXPERIMENTAL METHODS

Precipitation experiments were carried out in closed 250 ml vessels on calcite seeds in artificial seawater at 25°C (Fig. 1). Artificial seawater was prepared following Kester et al. (1967) but with five different magnesium concentrations, ranging from zero to typical seawater concentrations (0, 13.3, 26.5, 39.7, 53.0 mmol kg^{-1}) and with constant calcium concentration, typical for seawater (10 mmol kg^{-1}). At least two runs were carried out for each magnesium concentration. The *p*H electrode was calibrated before every run by NBS buffers at *p*H 4, 7, and 10. It is noted that NBS or NIST *p*H buffers should not be used for high-precision *p*H measurements in seawater (Wedborg et al., 1999). This is, however, of minor importance for the present study, as will be discussed in Sect. 3.1. At the beginning of each experiment 150 mg of calcite seeds were added to the solution and the vessel was closed with a negligible head space at the top of the vessel. It was carefully checked that the *p*H remained stable after the addition of the seeds. The *p*H was monitored every 20 s using a computer controlled autotitrator system (Chris Langdon, Private communication, see also Sanyal et al., 2000). The *p*H was then increased by repeatedly adding known amounts of base (0.1 N NaOH). In order to produce small increases in *p*H per addition (<0.05 *p*H units), small amounts of base were added (usually 15–100 μl). After each addition and establishment of chemical equilibrium, which takes less than 60 s (Zeebe et al., 1999), it was checked whether the *p*H remained stable or dropped over a period of approximately 5 minutes. The procedure was repeated until a continuous drop of *p*H was observed. A blank run without seeds was also conducted to make sure that the precipitation as seen before was indeed on seeds and not on the walls of the vessel or spontaneous precipitation. Even at *p*H 9.96 and seawater Mg^{2+} concentration, no drop of *p*H was observed without seeds. At $pH > 10$, spontaneous precipitation was observed.

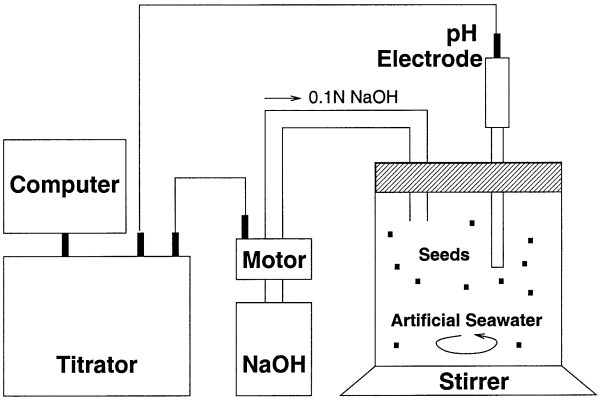

Fig. 1. Schematic view of the experimental setup used for inorganic precipitation experiments.

3. THEORETICAL CONSIDERATIONS

Calcium carbonate formation may be described by the overall reaction

$$Ca^{2+} + 2\,HCO_3^- \rightarrow CaCO_3 + CO_2 + H_2O. \qquad (1)$$

Precipitation of $CaCO_3$ leads to a decrease in total dissolved inorganic carbon (ΣCO_2)

$$\sum CO_2 = [CO_2] + [HCO_3^-] + [CO_3^{2-}],$$

where

$$[CO_2] = [CO_2(aq.)] + [H_2CO_3]$$

and to a decrease in total alkalinity (A_T), which, for the artificial seawater used in this study, is given by

$$A_T = [HCO_3^-] + 2\,[CO_3^{2-}] + [B(OH)_4^-] + [OH^-] - [H^+]$$

Because one carbon and one doubly charged calcium atom are removed from solution per molecule of $CaCO_3$ formed [reac-

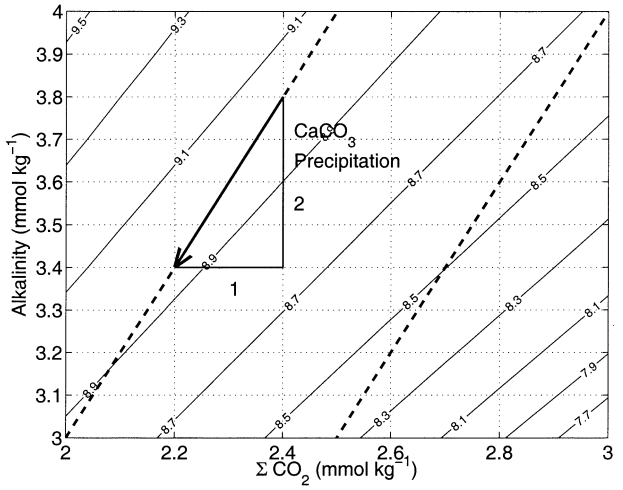

Fig. 2. Effect of $CaCO_3$ precipitation on seawater *p*H. The thin solid lines indicate contours of *p*H as a function of total dissolved inorganic carbon (ΣCO_2) and total alkalinity (A_T). When $CaCO_3$ is formed, ΣCO_2 and A_T are reduced by 1 and 2 units, respectively (dashed lines), and the *p*H decreases. The *p*H values shown are based on the NBS *p*H scale and were calculated using dissociation constants given by Mehrbach et al. (1973). The total boron concentration is 420 μmol kg^{-1}.

tion (1)], ΣCO_2 and A_T are reduced by one and two units, respectively, per unit of $CaCO_3$ formed. Roughly, the difference between A_T and ΣCO_2 is equal to the carbonate ion concentration which decreases as a result of $CaCO_3$ formation. The solution gets more acidic and the *p*H decreases. Precipitation and dissolution of $CaCO_3$ can therefore be recognized by monitoring the *p*H. Figure 2 shows contours of constant *p*H (NBS *p*H scale) as a function of ΣCO_2 and A_T. Also shown are lines of slope 2 indicating the change of the carbonate chemistry upon $CaCO_3$ formation. For example, the production of 0.5 mmol kg^{-1} $CaCO_3$ at $\Sigma CO_2 = 3$ mmol kg^{-1} and $A_T = 4$ mmol kg^{-1} leads to a decrease of *p*H from 8.66 to 8.35. In our experiments, the decrease in ΣCO_2 was deduced from the decrease of *p*H which was clearly detectable (see Sect. 4.1). The total decrease of ΣCO_2 in the course of an experiment was, however, negligible (usually $<0.2\%$ of ΣCO_2, see Sect. 3.2).

3.1. Dissociation Constants

All carbonate chemistry parameters in this paper were calculated using the dissociation constants originally given by Mehrbach et al. (1973). These constants, as well as the *p*H values measured in our experiments, are based on the NBS *p*H scale. This approach yields internal consistency between measured and calculated values. The NBS *p*H scale can be used here because (1) no high-precision determination of carbonate system parameters is required for the results of this study and (2) the differences in the dissociation constants of carbonic acid, K_1' and K_2', brought about by variations of the Mg^{2+} concentration are far more important than uncertainties arising from the use of NBS buffers. For example, at *p*H 8.2 and $\Sigma CO_2 = 2.33$ mmol kg^{-1} ($T = 25°C$, $S = 35$), the calculated carbonate ion concentration in seawater containing 53 mmol Mg^{2+} kg^{-1} is $\sim$250 μmol kg^{-1}, whereas only $\sim$150 μmol kg^{-1} are calculated for Mg-free seawater.

Table 1. Dissociation constants of carbonic acid at 25°C.[a]

$[Mg^{2+}]$ (mmol kg^{-1})	K_1' ($\times 10^6$)	K_2' ($\times 10^9$)
0.0	0.8449	0.4290
13.3	0.8839	0.5145
26.5	0.9222	0.5986
39.7	0.9611	0.6837
53.0	0.9999[b]	0.7689[b]

[a] Corrected for the effect of $[Mg^{2+}]$, see Ben-Yaakov and Goldhaber (1973).
[b] Mehrbach et al. (1973).

The values of K_1' and K_2' were corrected for the effect of varying Mg^{2+} concentration using sensitivity parameters given by Ben-Yaakov and Goldhaber (1973). The sensitivity parameters describe the relative change of the dissociation constants as a function of the magnesium concentration (cf. Garrels and Thompson, 1962; Mucci and Morse, 1984; Millero and Schreiber, 1982). Values for K_1' and K_2' at various Mg^{2+} concentrations are given in Table 1.

3.2. Precipitation Rate

For the interpretation of our experiments it is of great importance that the rate of inorganic precipitation on seeds is comparable to precipitation rates of biogenic calcification in planktonic foraminifera. The inorganic precipitation rate was similar in all experiments and decreased only slightly with increasing Mg^{2+} concentration (see Sect. 4.1). This is a direct result of our approach because the onset of precipitation was defined by the same decrease of *p*H over time for all experiments. (Note that at higher Mg^{2+} concentration, the critical *p*H and thus the corresponding CO_3^{2-} concentration are higher, as well.) In other words, the system determines the critical *p*H at which the inhibiting effect of Mg^{2+} on the precipitation rate is just compensated by higher CO_3^{2-} concentration.

The average drop of *p*H vs. time in our experiments was

$$\frac{\partial p\mathrm{H}}{\partial t} \simeq -0.12\ \mathrm{h}^{-1}. \tag{2}$$

Figure 2 shows that ΣCO_2 decreases on average by 0.5×10^{-3} mol kg^{-1} as *p*H decreases by roughly 0.25 units when $CaCO_3$ is formed (dashed lines). Thus,

$$\frac{\partial \sum \mathrm{CO}_2}{\partial p\mathrm{H}} \simeq 2 \times 10^{-3}\ \mathrm{mol\ kg}^{-1}. \tag{3}$$

Multiplying Eqns. (2) and (3) yields the change of ΣCO_2 due to precipitation on seeds in the vessel per hour:

$$\frac{\partial \sum \mathrm{CO}_2}{\partial t} \times M_v \simeq -0.12 \times 2 \times 10^{-3} \times 0.25 = -60\ \mu\mathrm{mol\ h}^{-1},$$

where $M_v \simeq 0.25$ kg is the weight of the seawater in the vessel. The decrease in ΣCO_2 now has to be related to the total surface area of the calcite seeds. We used 150 mg of calcite seeds with a grain size of $\sim$10 μm. Assuming a cubic shape of the crystals, the specific surface area can be estimated as $6/(2.7 \times$

10^6 g m^{-3} $\times$ 10 $\times$ 10^{-6} m) = 0.22 m^2 g^{-1} where the density of calcite $\rho_c = 2.7 \times 10^6$ g m^{-3} has been used. The total surface area therefore is $\sim$0.033 m^2. Finally, the inorganic precipitation rate R on seeds in our experiment is

$$R \simeq 60 \times 10^{-6} \times (0.033)^{-1} = 1.8 \times 10^{-3} \text{ mol m}^{-2} \text{ h}^{-1}.$$

Precipitation rates in planktonic foraminifera have been estimated to be about 1–4 $\times$ 10^{-3} mol m^{-2} h^{-1} (Carpenter and Lohmann, 1992; Lea et al., 1995). Thus, the inorganic precipitation rate of this study and biogenic precipitation rates in planktonic foraminifera are compatible. Based on data of other inorganic seeded precipitation experiments, the same conclusion was derived by Carpenter and Lohmann (1992).

It is important to note that the precipitation rates in foraminifera estimated by Carpenter and Lohmann (1992) are not based on the geometric surface are of the shell. Their values are based on a model including multiple cylindrical plaques and the porosity of the shell. Alternatively, one could use the BET surface area (Brunauer et al., 1938) of sediment samples determined by e.g., Honjo and Erez (1978). However, it appears unrealistic to assume that the BET area represents the correct surface area for calcite growth in living foraminifera. The BET area of empty shells from sediment samples yields the total surface area accessible to the adsorbate (e.g., N_2), i.e., including the inside of the shell and the cylindrical walls surrounding the pores. Yet, crystal growth in living foraminifera does not occur on this total area (e.g., Hemleben et al., 1977; Bé et al., 1979). If this was the case, pores would immediately be closed by growth in the tangential direction of the calcitic chamber/sphere. Rather, the main growth occurs in the radial direction while the outer part of the shell is primarily thickened and pores are left open. It therefore appears reasonable that the true surface area on which precipitation occurs in foraminifera is smaller than the BET area but larger than the geometric area. This is consistent with the Carpenter and Lohmann model. Considering that biogenic precipitation rates also vary appreciably and that inorganic precipitation rates may vary over several orders of magnitude [depending on variables such as the supersaturation, e.g., Zuddas and Mucci (1994)], the agreement between the inorganic precipitation rate of the present study and biogenic precipitation rates is quite satisfactory.

4. RESULTS

Before presenting the experimental results, it is necessary to explain what will be referred to as “precipitation” and “no precipitation.” Precipitation in our experiments refers to the formation of $CaCO_3$ at precipitation rates similar to biogenic precipitation rates in planktonic foraminifera. As discussed in Sect. 3.2, this leads to a decrease of *p*H vs. time of approximately -0.1 h^{-1} or -0.002 min^{-1}. If the precipitation rate is significantly smaller than this, no decrease of *p*H will be observed over several minutes. This will be referred to as “no precipitation.” (Note that the internal drift of the system was negligible over this time period.) Obviously, this case also includes conditions under which calcite may indeed be precipitated. However, the precipitation rate in this case is too small to be detected within the chosen time limit and is therefore much smaller than precipitation rates in planktonic foraminifera.

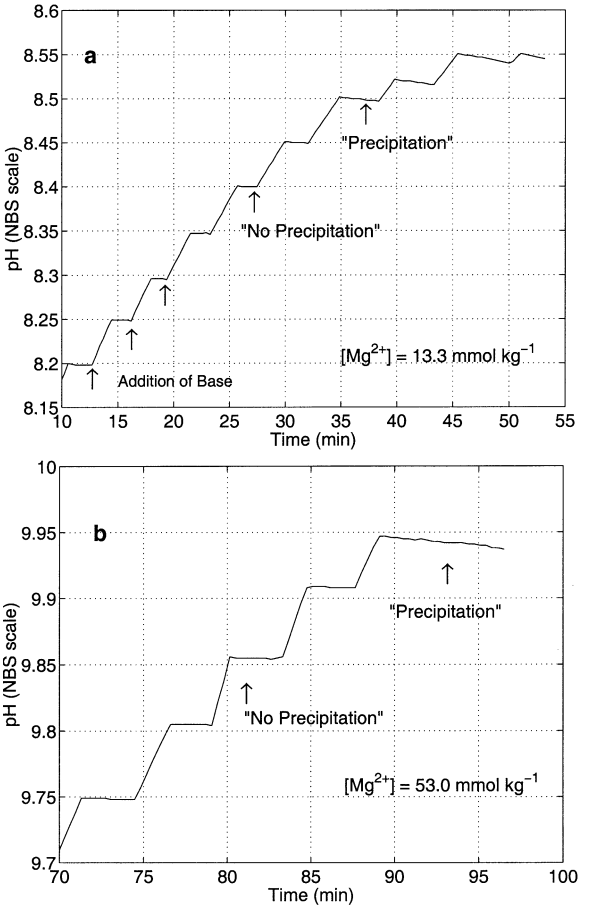

Fig. 3. Temporal development of the measured *p*H during the course of an experiment at (a) [Mg^{2+}] = 13.3 mmol kg^{-1} and (b) [Mg^{2+}] = 53.0 mmol kg^{-1}. Each addition of base results in an increase of *p*H. When the critical *p*H of $\sim$8.5 (a) and $\sim$9.95 (b) has been reached, calcite precipitation at a certain rate can be identified by the decrease of *p*H upon addition. For definition of “precipitation” and no “precipitation”, see the text. Note that in the slight drops of *p*H in (a) at t = 17, 19, 23, 32, and 38 min are artifacts arising from the addition process.

4.1. Critical *p*H

Typical graphs of the temporal evolution of the measured *p*H during the course of an experiment are shown in Fig. 3(a) ([Mg^{2+}] = 13.3 mmol kg^{-1}) and Fig. 3(b) ([Mg^{2+}] = 53 mmol kg^{-1}). Each addition of base results in an increase of *p*H [see arrows in the lower left corner in Fig. 3(a)]. Until the *p*H of the solution has reached a value of about 8.4, no drop of *p*H upon addition is observed over the considered period of time, indicating “no precipitation” at this *p*H. [Note that the slight drops of *p*H in Fig. 3(a) at the additions at t = 17, 19, 23, 32, and 38 min are artifacts resulting from electronic interference due to the addition process and do not indicate precipitation.] However, at *p*H 8.5, a continuous drop of *p*H over a time period of about 5 minutes is observed upon addition which indicates “precipitation.” The initial drop of *p*H calculated for the runs shown in Figs. 3(a) and 3(b) labeled “precipitation” are -0.085 and -0.081 h^{-1}, respectively.

The *p*H corresponding to the supersaturation required to trigger precipitation within the time interval considered (this

Table 2. Critical *p*H at various Mg^{2+} concentrations.

Experiment	$[Mg^{2+}]$ (mmol kg^{-1})	pH_{crit}[a] Run #1	Run #2
1	0	8.2	8.2
2	13.3	8.5	8.5
3	26.5	8.7	8.6
4	39.7	8.9	9.0
5	53.0	9.9	9.9

[a] Uncertainty in critical *p*H (NBS scale) is about ±0.05.

will be called the critical *p*H in the following) can be determined from Fig. 3(a) to be 8.5 ± 0.05 at $[Mg^{2+}] = 13.3$ mmol kg^{-1}. According to Fig. 3(b), the critical *p*H appears to be 9.9 ± 0.05 at $[Mg^{2+}] = 53$ mmol kg^{-1}. Using the procedure just described, the critical *p*H values at the various magnesium concentrations were determined for all experiments (Table 2).

Figure 4 shows the critical *p*H as a function of the magnesium concentration (left vertical axis). In magnesium free artificial seawater, a *p*H of 8.2 is sufficient to trigger calcite precipitation on seeds within a few minutes. However, the critical *p*H increases dramatically with the concentration of Mg^{2+} ions in solution. At a typical seawater magnesium concentration of 53.0 mmol kg^{-1}, the critical *p*H is about 9.9. This demonstrates the large effect of Mg^{2+} ions on the onset of calcite precipitation on time scales of minutes and at precipitation rates similar to biogenic calcification.

4.2. Critical Carbonate Ion Concentration

From the critical *p*H and the total dissolved inorganic carbon ($\Sigma CO_2 = 2.33$ mmol kg^{-1}), the critical carbonate ion concentration for the seawater solutions of various magnesium concentration can be calculated (Fig. 4, right vertical axis). This quantity increases from ~150 μmol kg^{-1} in magnesium free artificial seawater to more than 2 mmol kg^{-1} at seawater magnesium concentration. In other words, in order to maintain the same precipitation rate in seawater solutions containing 0 and 53.0 mmol Mg^{2+} kg^{-1}, the carbonate ion concentration has to increase by a factor of ~13. There are mainly two reasons for this dramatic increase.

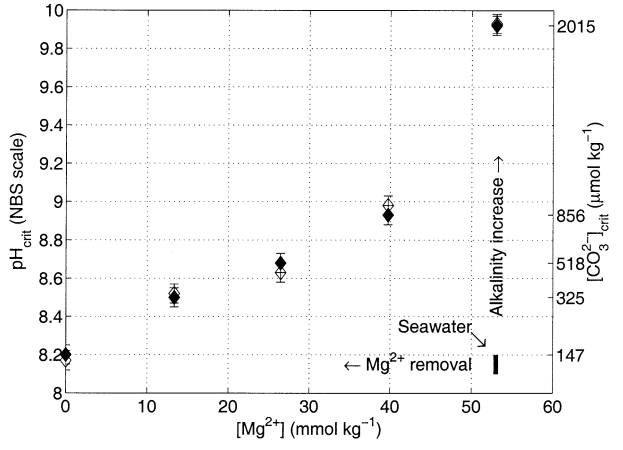

Fig. 4. Critical *p*H and critical carbonate ion concentration as a function of the magnesium concentration in solution (diamonds). The critical *p*H is the *p*H of the seawater solution of given magnesium concentration which is required to produce a precipitation rate typical for biogenic calcification. This quantity increases dramatically as $[Mg^{2+}]$ increases from 0 to typical seawater concentrations of 53 mmol kg^{-1}; $[CO_3^{2-}]$ is increasing by a factor of ~13. Closed and open diamonds indicate duplicate runs. Starting at typical surface seawater conditions (filled rectangle), one moves to the left if Mg^{2+} is removed and upward if alkalinity increases.

First, the total activity coefficient of CO_3^{2-} is reduced in the presence of Mg^{2+} ions. Magnesium and carbonate ions form strong ion pairs in seawater, thereby reducing the amount of free CO_3^{2-}. It can be calculated that about 70% of total CO_3^{2-} is associated with Mg^{2+}. As a result, the total activity coefficient of CO_3^{2-} drops by a factor of about 2 from 0.054 in Mg-free seawater to 0.029 in seawater containing 53 mmol kg^{-1} Mg^{2+} (Mucci and Morse, 1984), which in turn, reduces the saturation state of the solution and the precipitation rate of $CaCO_3$. The activity of carbonate ion is given by

$$\{CO_3^{2-}\} = \gamma^T_{CO_3^{2-}} [CO_3^{2-}]$$

where $\gamma^T_{CO_3^{2-}}$ is the total activity coefficient of CO_3^{2-}, and $[CO_3^{2-}]$ is the stoichiometric concentration of the carbonate ion. Thus, in order to maintain a constant activity of CO_3^{2-} in the presence and absence of seawater Mg^{2+}, the concentration of CO_3^{2-} has to increase roughly by a factor of 2.

Second, and most important, magnesium ions are incorporated into the crystal structure of calcite, thereby changing the morphology of the crystal and reducing the calcitc growth rate (e.g., Berner, 1975; Mucci and Morse, 1983; Zhang and Dawe, 2000). Davis et al. (2000) recently suggested that calcite growth is inhibited by enhanced mineral solubility through magnesium incorporation.

In summary, the presence of Mg^{2+} tends to reduce the precipitation rate of calcite by (1) reducing the concentration of free CO_3^{2-} and (2) increasing the calcite solubility through Mg^{2+} incorporation into the crystal. In order to compensate for these effects and to keep a constant precipitation rate throughout our experiments, the carbonate ion concentration had to increase by a factor of ~13 as the magnesium concentration increased from 0 to 53.0 mmol kg^{-1}.

4.3. Alkalinity Added

In every experiment, not only the *p*H but also the added amount of base was recorded as a function of time. This enables us to calculate the total alkalinity added to the system until the critical *p*H was reached. It is instructive to discuss this issue here for two reasons. First, the total alkalinity added is very useful for the interpretation of our results (Sect. 5). Second, it allows a cross-check of the results obtained directly from the experimental protocol and the results obtained from calculations of carbonate system parameters.

As an example, consider Experiment 4, run #1 (see Table 2). The total amount of base added in this experiment was 2.95 ml. Because 0.1 N NaOH was used, the total alkalinity added is 0.295 mmol. With the mass of the seawater in the vessel being ~0.25 kg, the total alkalinity added per kg is ~1.18 mmol kg^{-1}. On the other hand, during the course of the experiment the measured *p*H increased from 7.70 to 8.97. With ΣCO_2 =

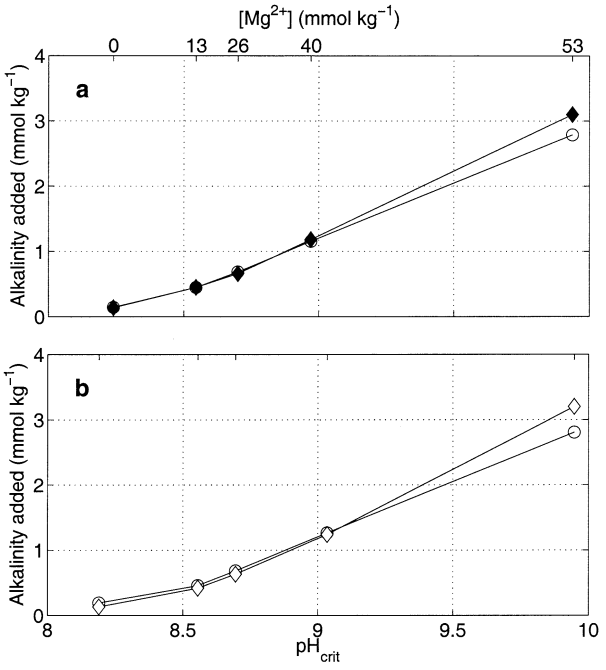

Fig. 5. Total alkalinity added until the critical *p*H was reached in each experiment. Diamonds indicate A_T added as calculated from the amount of base added, while open circles indicate A_T added as calculated from the measured increase in *p*H and $\Sigma CO_2 = 2.33$ mmol kg^{-1}. Dissociation constants by Mehrbach et al. (1973), corrected for the effect of [Mg^{2+}] were used (Ben-Yaakov and Goldhaber, 1973). (a) Run #1; (b) Run #2.

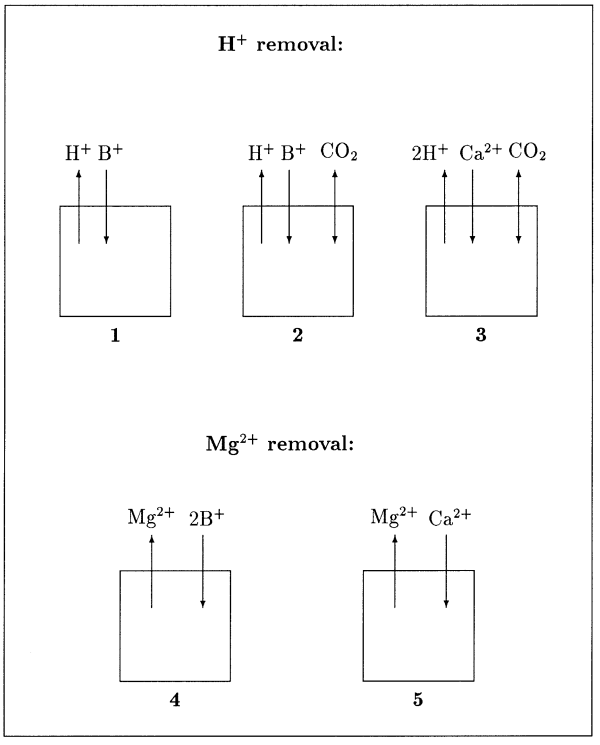

Fig. 6. Schematic illustration of different calcification scenarios. Each box represents a closed volume of seawater in which the concentrations of H^+, Mg^{2+}, and Ca^{2+} are manipulated. For example, in Scenario 1, H^+ is removed and electroneutrality is maintained by simultaneous influx of a cation B^+ or release of an anion A^- (not shown) for each proton removed; the system is closed to CO_2. In Scenario 2 and 3, the system is open to CO_2. Scenario 3 and 5 assume that H^+ and Mg^{2+}, respectively, are removed, while Ca^{2+} is taken up. Note that for the scenarios considered here, H^+ removal changes the alkalinity, whereas Mg^{2+} removal does not.

2.33 mmol kg^{-1} and using dissociation constants given in Table 1, one calculates an increase of total alkalinity of 1.15 mmol kg^{-1}. Thus, the two approaches yield quite similar results, considering the fact that an error of only 3% in the amount of base added would explain the differences between the two calculations. Figures 5(a) and 5(b) show the total alkalinity added as determined directly from the addition of base (diamonds) and as calculated from the increase in *p*H (circles) as a function of the critical *p*H at the various magnesium concentrations. Closed diamonds [Fig. 5(a)] and open diamonds [Fig. 5(b)] indicate duplicate runs.

5. MODELING OF CALCIFICATION SCENARIOS

The results presented in the preceding section can be used to investigate the inorganic basis of potential calcification strategies. First, our results demonstrate that removal of Mg^{2+} ions from seawater has a large effect on the critical *p*H necessary to trigger calcite precipitation on seeds at biogenic precipitation rates (Fig. 4). If magnesium is completely removed from the artificial seawater, calcite precipitation can be triggered at *p*H 8.2, a value close to the observed *p*H value of the surface ocean. Alternatively, if the magnesium concentration is not manipulated at all the *p*H must be increased to a value of about 9.9 to trigger calcite precipitation. (Note that on longer time scales and higher solid:solution ratios calcification can be initiated at much lower *p*H, see Introduction.)

We shall now discuss how "cost-effective" the two strategies are when expressed in terms of moles of Mg^{2+} and H^+ ions to be removed from solution in order to initiate calcite precipitation. We consider a volume of seawater at *p*H 8.2 closed to ion exchange with the exception of Mg^{2+} and H^+ ions. Electroneutrality may be maintained by simultaneous influx of conservative cations or release of conservative anions. As a result, H^+ removal changes the alkalinity because the concentration of conservative ions in the volume is affected. In contrast, Mg^{2+} removal does not change the alkalinity. In the following, five different scenarios will be compared which include the effect of CO_2 diffusion and Ca^{2+} influx (Fig. 6, cf. also ter Kuile, 1991). Ion transport systems which may facilitate ion transport across biological membranes in nature are discussed in Sect. 6.2.

5.1. Scenarios 1 and 4

Two end-member scenarios can be compared in which only Mg^{2+} and only H^+ ions are manipulated. The number of moles of Mg^{2+} ions to be removed at *p*H = 8.2 to initiate calcite precipitation is simply 53 mmol kg^{-1} (Fig. 4). On the other hand, the number of moles of H^+ ions to be removed is approximately 3 mmol kg^{-1} (Fig. 5). Assuming that the energy required for the removal of 1 mol Mg^{2+} and 2 mol H^+ is approximately the same, a calcifying organism would need about 35 times more energy for magnesium removal than for

proton removal in order to initiate calcite precipitation. (Note that this estimate may vary depending on the assumed energy requirement, see Sec. 6.) It appears that removal of H^+ ions is much more effective than removal of Mg^{2+} ions. However, this statement may need to be revised because two important aspects have so far been neglected in our discussion: the permeability of biological membranes to CO_2 and the role of calcium.

5.2. System Open to CO_2 (Scenario 2)

In nature, a calcification system discussed above might be realized by a membrane enclosing a volume of seawater in which calcite is precipitated. While membranes are usually impermeable to ions, they are highly permeable to neutral molecules such as H_2O and CO_2 that can diffuse rather freely across membranes. This has important consequences for one of the potential strategies discussed here. If calcite precipitation is brought about by H^+ removal, the internal *p*H of the enclosed volume has to increase significantly over the *p*H of the surrounding medium. As a result, the CO_2 concentration in the volume decreases, creating a CO_2 gradient across the membrane which causes a net diffusional flux from the ambient medium into the enclosed volume. Addition of CO_2 acts like addition of acid, therefore counteracting the removal of H^+. As a result, additional energy is necessary in order to maintain a high internal *p*H.

The CO_2 flux due to diffusion across the membrane per unit area can be estimated by

$$F = P\,(c_e - c_i),$$

where $P \simeq 1 \times 10^{-5}$ m s^{-1} $= 3.6 \times 10^{-2}$ m h^{-1} is the permeability of the membrane to CO_2 (e.g., Sültemeyer and Rinast, 1996), and c_e and c_i are the external and internal CO_2 concentrations, respectively. While c_e is set by the carbonate chemistry of the surrounding seawater, c_i is a function of the *p*H of the enclosed volume. The higher the internal *p*H, the larger the CO_2 gradient and thus the diffusional flux. Diffusion of CO_2 into the volume leads to an increase of ΣCO_2 with time. Assuming plane geometry, $\partial\Sigma CO_2/\partial t$ is given by

$$\frac{\partial \Sigma CO_2}{\partial t} = \frac{P}{d}\,(c_e - c_i),$$

where d is the thickness of the enclosed volume (perpendicular to the plane of the membrane). Assuming a high internal *p*H ($c_i \simeq 0$), $c_e = 10^{-5}$ mol kg^{-1}, and $d = 10^{-5}$ m,

$$\frac{\partial \Sigma CO_2}{\partial t} = 3.6 \times 10^{-2} \times 10^{-5}/10^{-5} = 36 \text{ mmol kg}^{-1}\,\text{h}^{-1}.$$

Although a first approximation, this is an important result. At high internal *p*H, there is a large flux of CO_2 into the enclosed volume and thus a large increase of ΣCO_2 with time. The magnitude of the flux is not negligible because it would entirely change the carbonate chemistry of the calcifying fluid over the period of 1 hour.

The most uncertain parameter in our model is d, the dimension of the enclosed volume of seawater. Because the model is partly based on a thought experiment, parameters such as d cannot simply be taken from the literature. However, if the model is applicable to calcification in planktonic foraminifera, d should be of the order of the thickness of the calcite shell (~5–20 μm, Hemleben et al., 1989). Figure 7 shows values of $\partial\Sigma CO_2/\partial t$ as a function of the internal *p*H and different values of d at $\Sigma CO_2 = 2.33$ mmol kg^{-1} and $pH_e = 8.2$. Even for $d = 20$ μm, $\partial\Sigma CO_2/\partial t$ is large reaching about 20 mmol kg^{-1} h^{-1} at high internal *p*H which in turn would tend to decrease the internal *p*H rapidly. In summary, the H^+ -removal strategy would require additional energy in order to maintain a high internal *p*H and thus favorable conditions for calcification. On the other hand, the increase of ΣCO_2 resulting from CO_2 influx would increase $[CO_3^{2-}]$ and thus the saturation state, which would partly compensate for the decrease in *p*H. This is discussed in the following.

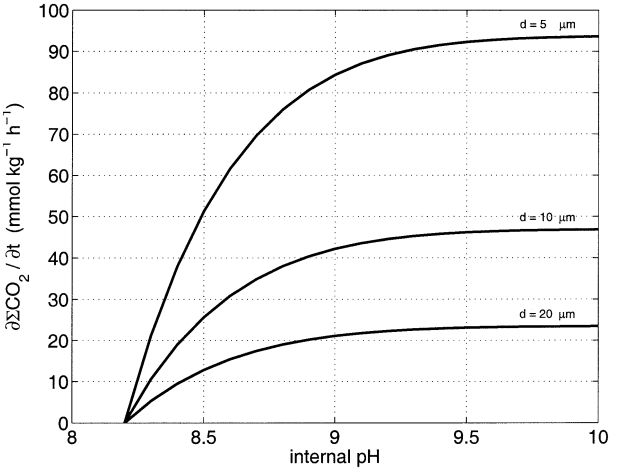

Fig. 7. Increase of ΣCO_2 with time ($\partial\Sigma CO_2/\partial t$) as a function of the *p*H of the enclosed volume of seawater (internal *p*H) when CO_2 diffusion across the membrane is taken into account (see text). As the internal *p*H increases, the internal CO_2 decreases. This produces a flux into the enclosed volume that raises ΣCO_2 with time. $\partial\Sigma CO_2/\partial t$ depends on the parameter d, the thickness of the enclosed volume (perpendicular to the plane of the membrane), for which different values are indicated.

5.2.1. *The minimum energy case*

The considerable diffusional flux of CO_2 across the membrane would tend to equilibrate c_i and c_e. We shall now discuss the case in which $c_i = c_e$, i.e., the internal and external CO_2 concentration are equal at any given time during H^+ removal. This might be referred to as the minimum energy case because no energy is used to maintain the CO_2 gradient that results from the H^+ gradient across the membrane. The seawater system considered thus has a constant CO_2 concentration and is open to total alkalinity and total dissolved inorganic carbon. Any increase of A_T brought about by removal of H^+ from the enclosed volume is followed by a subsequent influx of CO_2 until $c_i = c_e$ is restored. Figure 8 shows carbonate system parameters for this system. Starting at external seawater conditions, say *p*H = 8.2 and $[CO_2] = 11$ μmol kg^{-1}, one moves along the line of constant CO_2 as A_T increases. When the internal *p*H has reached 8.7, the carbonate ion concentration is about 2 mmol kg^{-1}, which is approximately equal to the carbonate ion concentration necessary to trigger calcite precipitation at seawater magnesium concentration (Fig. 4). The total

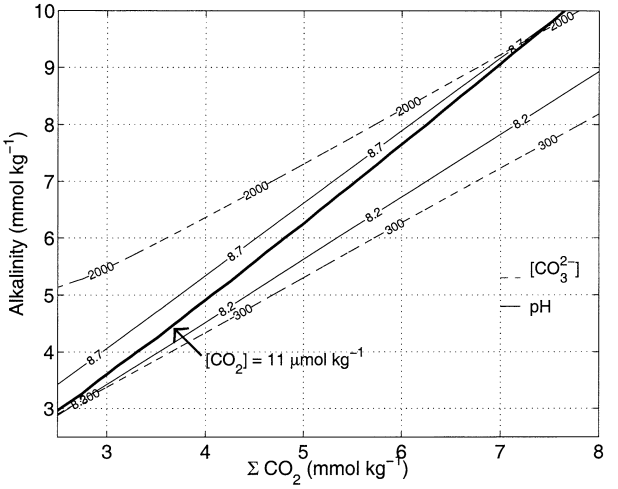

Fig. 8. Carbonate chemistry parameters for a model in which H^+ is removed from the enclosed seawater and CO_2 is constant (bold solid line). Thin solid and dashed lines indicate contours of constant *p*H and $[CO_3^{2-}]$, respectively. Starting at *p*H 8.2 (lower left corner), one moves along the line of constant CO_2 until a critical carbonate ion concentration of about 2000 μmol kg^{-1} is reached (upper right corner) at which calcite precipitation is triggered. At this point removal of H^+ has led to an increase of total alkalinity to more than 9 mmol kg^{-1}.

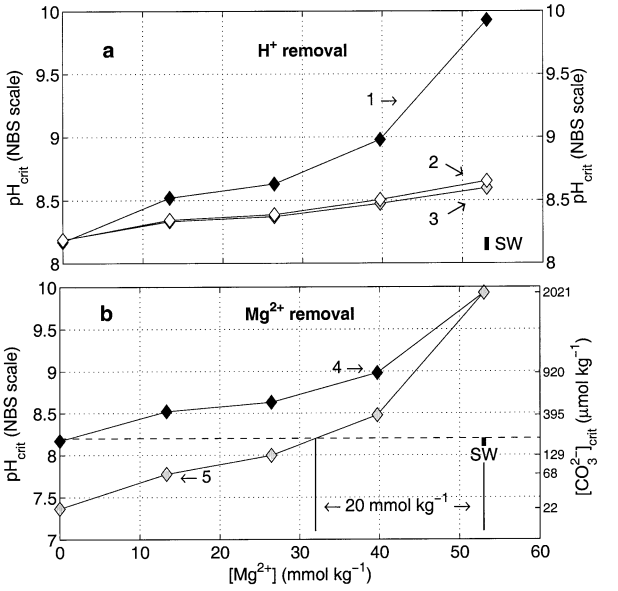

Fig. 9. Critical *p*H and carbonate ion concentrations for the different scenarios as a function of the Mg^{2+} concentration (cf. Fig. 6). (a) Critical *p*H for H^+ removal. (1) System closed to CO_2, (2) system open to CO_2, (3) CO_2 diffusion plus Ca^{2+} exchange. (b) Critical *p*H and $[CO_3^{2-}]$ for Mg^{2+} removal. (4) Mg^{2+} removal, (5) Mg^{2+} removal plus Ca^{2+} uptake. The small filled rectangle, denoted by SW, indicates typical surface seawater conditions. If the initial chemistry of the calcifying fluid corresponds to SW, then the distances to the respective graphs indicate Mg^{2+} decrease (horizontal axes) and *p*H increase (vertical axes) required to initiate calcite precipitation for the different scenarios.

alkalinity at this point is roughly 10 mmol kg^{-1}, demonstrating that the number of H^+ ions that have to be removed from solution in order to trigger calcite precipitation in this system is ~7 mmol kg^{-1}. As said above, this estimate refers to the minimum energy case. In Fig. 9(a), the critical *p*H for Scenario 1 (closed system, closed diamonds) and Scenario 2 (open system, open diamonds) are compared. The critical *p*H for the open system is much lower than for the closed system. Note that the critical carbonate ion concentration is constant in the two cases.

5.3. The Role of Calcium (Scenarios 3 and 5)

Another aspect that may significantly alter our estimate of cost-effectiveness is the role of Ca^{2+} ions. Provided that our model of ion exchange indeed applies to planktonic foraminifera, it is likely that, for example, the cations which are exchanged for H^+ ions are Ca^{2+} ions. On the other hand, Mg^{2+} removal may be accompanied by simultaneous influx of Ca^{2+}. These strategies would at the same time reduce inhibitory effects by magnesium or raise the saturation state by increasing $[CO_3^{2-}]$, *and* raise the saturation state by increasing $[Ca^{2+}]$. The influence of the calcium concentration on the critical *p*H and CO_3^{2-} concentration required to initiate precipitation can be estimated as follows. Let the critical saturation state of the seawater solution found in our experiments be K^*_{crit}:

$$K^*_{crit} = [Ca^{2+}]_{sw} \times [CO_3^{2-}]_{crit},$$

where $[Ca^{2+}]_{sw} = 10$ mmol kg^{-1} is the calcium concentration—close to natural seawater concentration—which was held constant in all experiments. What happens if calcium is varied? If a constant K^*_{crit} is required for a given precipitation rate, then we can always write

$$[Ca^{2+}]_{crit} \times [CO_3^{2-}]'_{crit} = [Ca^{2+}]_{sw} \times [CO_3^{2-}]_{crit}$$

where $[Ca^{2+}]_{crit}$ is the critical calcium concentration corresponding to $[CO_3^{2-}]'_{crit}$, the critical carbonate ion concentration at this calcium concentration. Thus, $[CO_3^{2-}]'_{crit}$ is given by

$$[CO_3^{2-}]'_{crit} = K^*_{crit}/[Ca^{2+}]_{crit}. \quad (4)$$

Using Eq. (4), the effect of calcium on the critical *p*H and the critical carbonate ion concentration can be calculated for the case of H^+ and Mg^{2+} removal, respectively (Scenarios 3 and 5).

In the case of H^+ removal we may assume that the alkalinity increase is brought about by exchanging two H^+ ions for one Ca^{2+} ion (Scenario 3). The corresponding increase of $[Ca^{2+}]$ does not only affect the alkalinity but also the saturation state: as $[Ca^{2+}]$ increases, the critical carbonate ion concentration decreases. Using the results for the critical carbonate ion concentration at $[Ca^{2+}]_{sw} = 10$ mmol kg^{-1} shown in Fig. 4, $[CO_3^{2-}]'_{crit}$ and $[Ca^{2+}]_{crit}$ at each Mg^{2+} concentration can then be found by means of Eq. (4) and a simple iteration procedure. The results are shown in Fig. 9(a) (gray diamonds). Compared to the open system (Scenario 2), the additional effect of calcium does not change the critical *p*H dramatically. However, $[CO_3^{2-}]_{crit}$ decreases by up to 450 μmol kg^{-1} because $[Ca^{2+}]$ increases (values not shown).

In the case of Mg^{2+} removal, Mg^{2+} ions are removed and Ca^{2+} ions are taken up, say at a stoichiometry of 1:1 (Scenario 5). For instance, if $[Mg^{2+}]$ is decreased from typical seawater

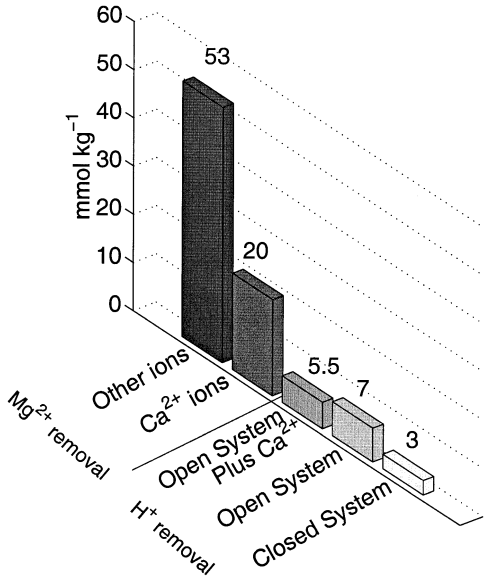

Fig. 10. Summary of the number of moles to be removed from solution in order to initiate calcite precipitation at biogenic precipitation rates. It appears that, regardless of the scenario considered, H^+ removal (alkalinity increase) is more cost-effective than Mg^{2+} removal. If the energy necessary to remove one mole Mg^{2+} and two moles H^+ is identical, then Mg^{2+} removal is even more expensive than the numbers suggest.

concentration of 53 mmol kg^{-1} by 13 mmol kg^{-1} [Fig. 9(b)], then [Ca^{2+}] is increasing from 10 to 23 mmol kg^{-1}. This produces a substantial increase of the saturation state. As a result, if Mg^{2+} ions are replaced by Ca^{2+} ions the number of moles of Mg^{2+} ions that need to be removed is reduced to ~20 mmol kg^{-1} [Fig. 9(b)].

6. DISCUSSION

The "cost-effectiveness" of the different scenarios is summarized in Fig. 10. By including CO_2 diffusion and Ca^{2+} exchange, we have shown that the number of moles of H^+ to be removed is about 7 and 5.5 mmol kg^{-1}, respectively. These numbers are larger than ~3 mmol kg^{-1} initially estimated for the system closed to CO_2 and ignoring calcium. However, these numbers are still significantly smaller than the number of moles of Mg^{2+} ions to be removed in order to initiate calcite precipitation at *p*H 8.2. Roughly, 53 and 20 mmol kg^{-1} can be estimated for Mg^{2+} removal, where the latter case includes calcium uptake. If the energy required for removal of one mole Mg^{2+} is the same as for the removal of two moles H^+, then Mg^{2+} removal is even more expensive than these numbers suggest. [Although energy requirements of H^+–ATPases for intracellular *p*H regulation in animals are known (e.g., Pörtner et al., 2000), the energy source for active Mg^{2+} transport is controversial, see Sect. 6.2.]

Provided that our results for inorganic precipitation are applicable to biogenic calcification, the following conclusion can be drawn. From a purely energetic point of view, removal of H^+ ions appears to be much more effective than removal of Mg^{2+} ions. In other words, if cost-effectiveness is the only criterion considered, H^+ removal is the better strategy for "house building." However, it is a truism that the cheaper house is not necessarily the better one. It was already mentioned in the introduction that the calcite shells of planktonic foraminifera have magnesium concentrations about a factor of 10 smaller than inorganic calcite. This observation strongly suggests that these organisms have control over the chemical composition of the calcifying fluid and in particular may reduce the magnesium concentration at the site of calcification. It therefore appears unlikely that cost-effectiveness is the only variable determining the strategies of planktonic foraminifera for shell formation. Another criterion might be the thermodynamic stability of the carbonates precipitated. For example, low-magnesian calcite is less soluble than high-magnesian calcite (e.g., Mucci and Morse, 1984; Morse and Mackenzie, 1990).

From the above discussion it is inferred that there is evidence that H^+ and Mg^{2+} removal are potential strategies of planktonic foraminifera to initiate calcite precipitation. In the light of our laboratory experiments, H^+ removal appears to be a useful strategy because it is cost-effective. Active manipulation of Mg^{2+} at the site of calcification may be useful considering the thermodynamic stability of low-magnesian vs. high-magnesian calcite. However, Mg^{2+} removal appears to be very expensive.

6.1. Photosynthesis

There is little doubt that photosynthesis of symbiotic algae in foraminifera enhances calcification (e.g., Anderson and Faber, 1984; Lea et al., 1995). The usual interpretation of this phenomenon is that photosynthesis raises the *p*H and carbonate ion concentration in the microenvironment of the foraminifer which in turn increases the precipitation rate. It is therefore likely that the manipulation of *p*H at the site of calcification is a common strategy for calcification in foraminifera as well. Interestingly, the calculated *p*H values required to initiate calcite precipitation in Scenarios 2 and 3 [Fig. 9(a)] correspond very well to measured and modeled *p*H values in symbiont-bearing foraminifera at the surface of the calcite shell (Rink et al., 1998; Wolf-Gladrow et al., 1999).

Regarding links between photosynthesis and calcification it is important to note that there are also nonsymbiotic foraminifera that produce low-magnesian calcite with calcification rates similar to those of symbiotic species. Moreover, symbiotic species also calcify during the night (Hemleben et al., 1989; Anderson and Faber, 1984; Lea et al., 1995). In other organisms such as corals and coccolithophores calcification has been shown to occur in the dark, as well (e.g., Simkiss and Wilbur, 1989; van der Wal et al., 1987; Linschooten et al., 1991). Thus, while light and photosynthesis can greatly enhance calcification rates, photosynthesis is not vital to mineral deposition. Because we aim to understand the fundamentals of calcification mechanisms in this paper, we have so far ignored photosynthesis in our estimates of cost-effectiveness.

Photosynthesis efficiently removes protons and may help to increase the *p*H of the calcifying fluid. As a result, photosynthesis can stimulate calcification (theories that suggest the opposite are controversial, see e.g., Gattuso et al., 2000). Photosynthesis may therefore reduce the cost for H^+ removal. This would make H^+ removal an even more cost-effective strategy than Mg^{2+} removal and our main conclusion would hold for both symbiotic and nonsymbiotic species. It is well known that

Mg^{2+} is a center metal ion in chlorophyll (e.g., Kendrick et al., 1992). One may speculate whether in photosynthetic or symbiotic organisms Mg^{2+} uptake during chlorophyll synthesis is linked to Mg^{2+} removal during calcification. This, however, requires that Mg^{2+} ions that are removed from the calcifying fluid at the site of calcification directly influence Mg^{2+} uptake at the site of chlorophyll synthesis within the chloroplast. Such a scenario appears unlikely, at least in foraminifera, due to the spatial separation between host and symbionts. Unfortunately, our knowledge of the role and transport of Mg^{2+} is very limited (Flatman, 1991; Maguire et al., 1992) which makes it impossible to quantify any mutual benefits between photosynthesis and calcification regarding Mg^{2+}.

6.2. Ion Transport Across Membranes

The scenarios considered to illustrate possible strategies to initiate calcite precipitation in foraminifera (Fig. 6) are hypothetical. An important feature of our scenarios is the transport of ions across membranes. We shall therefore discuss potential ion transport systems which may facilitate ion influx or extrusion in nature. It should be pointed out that we did not find any detailed studies on ion transport systems in foraminifera in the literature. It therefore remains speculative whether the ion transport systems found in other organisms (discussed below) are active in foraminifera or not.

In Scenarios 1 to 3, protons and calcium ions are transported across the membrane. Proton transport across membranes by means of H^+–ATPase is a widespread phenomenon which has been observed in animals, plants, and bacteria; Ca^{2+}–ATPase is common in animal cells (e.g., Lehninger, 1982; Evans and Graham, 1989). It is therefore possible, but by no means certain, that foraminifera may use H^+–ATPase and Ca^{2+}–ATPase in order to transport these ions across a membrane enclosing the calcifying fluid. If so, they may be able to actively increase *p*H and the calcium concentration in order to initiate calcite precipitation.

In contrast to proton and calcium transport systems, magnesium transport systems are less well understood. Transmembrane flux of Mg^{2+} has been deduced in, e.g., squid axons, human red cells, chicken, bacteria, in the medicinal leech, paramecia and other organisms (for review, see Flatman, 1984; Flatman, 1991). The energy source for active Mg^{2+} transport is controversial. Mainly, two different mechanisms are discussed. One of them is a Na^+–Mg^{2+} antiport which obtains all of its energy from the Na^+ and Mg^{2+} gradients, the other one is a magnesium pump using energy from ATP hydrolysis. With respect to the Na^+–Mg^{2+} antiport, there is considerable variation in transport stoichiometry. Either 1, 2, or 3 Na^+ ions may be exchanged for 1 Mg^{2+} ion (e.g., Flatman, 1991; Günzel and Schlue, 1997). A promising approach to understanding Mg^{2+} transport is molecular genetics. For example, Maguire et al. (1992) report genetic evidence for a Mg^{2+} transporting ATPase in the bacterium *Salmonella typhimurium*. Finally it is noted that Preston (1998) found transmembrane Mg^{2+} currents in the protozoan *paramecium tetraurelia*.

The bottom line is that H^+, Ca^{2+}, and Mg^{2+} ion transport systems have been detected in various organisms. Whether or not these systems facilitate ion transport in foraminifera to manipulate *p*H, calcium, and magnesium in order to initiate calcite precipitation, remains to be tested.

7. SUMMARY AND CONCLUSIONS

We have investigated the influence of magnesium and *p*H on the onset of inorganic calcite precipitation on seed crystals at typical biogenic precipitation rates. The *p*H required to initiate precipitation increased by ~1.7 units when the concentration of Mg^{2+} in solution increased from 0 to 53 mmol kg^{-1}. This corresponds approximately to a 13-fold increase of the carbonate ion concentration. The experimental results were used to compare two potential strategies of planktonic foraminifera to initiate calcite precipitation: removal of Mg^{2+} and H^+ ions. If our results are applicable to biogenic calcification it appears that H^+ removal is much more effective than Mg^{2+} removal.

This result is enigmatic because foraminifera produce low-magnesian calcite indicating that they may actively reduce the magnesium concentration at the site of calcification. We believe that it is worthwhile attempting to solve this puzzle in the future. First, considering the importance of biogenically produced $CaCO_3$ for the global carbon cycle, it is pitiful that we do not entirely understand the process of biogenic precipitation. Second, Mg/Ca ratios in foraminifera are now increasingly used to reconstruct temperatures of past oceans. In order to evaluate the potential of this proxy, we should understand how foraminifera control the magnesium content of their shells.

Acknowledgments—We thank Chris Langdon who lent us his autotitrator system. Discussions with Jelle Bijma, Wally Broecker, Joe Ortiz, Hans-Otto Pörtner, Ulf Ricbesell, and Ingrid Zondervan were useful and are gratefully acknowledged. We thank Jonathan Erez, Alfonso Mucci, and an anonymous reviewer for their reviews. R. E. Z. was sponsored by the Deutsche Forschungsgemeinschaft.

Associate editor: A. Mucci

REFERENCES

Anderson O. R. and Faber, W. W., Jr. (1984) An estimation of calcium carbonate deposition rate in a planktonic foraminifer *Globigerinoides sacculifer* using ^{45}Ca as a tracer: A recommended procedure for improved accuracy. *J. Foraminiferal Res.* **14,** 303–308.

Bé A. W. H., Hemleben Ch., Anderson O. R., and Spindler, M. (1979) Chamber formation in planktonic foraminifera. *Micropaleontology* **25,** 294–307.

Ben-Yaakov S. and Goldhaber M. B. (1973) The influence of sea water composition on the apparent constants of the carbonate system. *Deep-Sea Res.* **20,** 87–99.

Berner R. A. (1975) The role of magnesium in the crystal growth of calcite and aragonite from sea water. *Geochim. Cosmochim. Acta* **39,** 489–504.

Berner R. A., Westrich J. T., Graber R., Smith J., and Martens Ch. S. (1978) Inhibition of aragonite precipitation from supersaturated seawater: A laboratory and field study. *Am. J. Sci.* **278,** 816–837.

Brunauer S., Emmett P. H., and Teller E. (1938) Adsorption of gases in multimolecular layers. *J. Am. Chem. Soc.* **60,** 309–319.

Carpenter S. J. and Lohmann K. C. (1992) Sr/Mg ratios of modern marine calcite: Empirical indicators of ocean chemistry and precipitation rate. *Geochim. Cosmochim. Acta* **56,** 1837–1849.

Chave K. E. and Suess E. (1970) Calcium carbonate saturation in seawater: Effects of dissolved organic matter. *Limnol. Oceanogr.* **15,** 633–637.

Davis K. J., Dove P. M., and De Yoreo J. J. (2000) The role of Mg^{2+} as an impurity in calcite growth. *Science* **290,** 1134–1137.

Evans W. H. and Graham J. M. (1989) *Membrane structure and function, 'In* Focus'-series (ed. D. Rickwood), p. 86. IRL Press at Oxford University Press.

Flatman P. W. (1984) Magnesium transport across cell membranes. *J. Membrane Biol.* **80,** 1–14.

Flatman P. W. (1991) Mechanisms of magnesium transport. *Ann. Rev. Physiol.* **53,** 259–271.

Garrels R. M. and Thompson M. E. (1962) A chemical model for seawater at 25°C and one atmosphere total pressure. *Am. J. Sci.* **260,** 57–66.

Gattuso J.-P., Reynaud-Vaganay S., Furla P., Romainc-Lioud S., Jaubert J., Bourge I., and Frankignoulle M. (2000) Calcification does not stimulate photosynthesis in the zooxanthellate scleractinian coral *Stylophora pistillata. Limnol. Oceanogr.* **45,** 246–250.

Günzel D. and Schlue W.-R. (1997) Intracellular Mg^{2+} is regulated by 1 Na^+/1 Mg^{2+} antiport in neurones of an invertabrate central nervous system. *Electrochim. Acta* **42,** 3207–3215.

Hemleben Ch., Spindler M., and Anderson O. R. (1989) Modern planktonic foraminifera, p. 209. Springer-Verlag.

Hemleben Ch., Bé A. W. H., Anderson O. R., and Tuntivate S. (1977) Test morphology, organic layers and chamber formation of the planktonic foraminifer *Globorotalia Menardii* (d'Orbigny). *J. Foraminiferal Res.* **7,** 1–25.

Honjo S and Erez J. (1978) Dissolution rates of calcium carbonate in the deep ocean; an in-situ experiment in the North Atlantic ocean. *Earth Planet. Sci. Lett.* **40,** 287–300.

Kendrick M. J., May M. T., Plishka M. J., and Robinson K. D. (1992) *Metals in Biological Systems.* Ellis Horwood.

Kester D. R., Duedall I. W., Connors D. N., and Pytkowicz R. M. (1967) Preparation of artificial seawater. *Limnol. Oceanogr.* **12,** 176–179.

Lehninger A. L. (1982) *Principles of Biochemistry.* Worth Publishers Inc.

Lea D. W., Martin P. A., Chan D. A., and Spero H. J. (1995) Calcium uptake and calcification rate in the planktonic foraminifer *Orbulina universa. J. Foraminiferal Res.* **25,** 14–23.

Lea D. W., Mashiotta T. A., and Spero H. J. (1999) Controls on magnesium and strontium uptake in planktonic foraminifera determined by live culturing. *Geochim. Cosmochim. Acta.* **63,** 2369–2379.

Lebrón I. and Suárez D. L. (1998) Kinetics and mechanisms of precipitation of calcite as affected by Pco_2 and organic ligands at 25°C. *Geochim. Cosmochim. Acta* **62,** 405–416.

Linschooten C., van Bleijswijk J. D. L., van Emburg P. R., de Vrind J. P. M., Kempers E. S., Westbroek P., and de Vrind-de Jong E. W. (1991) Role of the light–dark cycle and medium composition on the production of coccoliths by Emiliania huxleyi (IIaptophyceae). *J. Phycol.* **27,** 82–86.

Lowenstam H. A. and Weiner S. (1989) *On Biomineralization.* Oxford University Press.

Maguire M. E., Snavely M. D., Leizman J. B., Gura S., Bagga D., Tao T., and Smith D. L. (1992) Mg^{2+} transporting P-type ATPases of *Salmonella typhimurium*. In *Ion-Motive ATPases: Structure, Function, and Regulation* (eds, A. Scarpa, E. Carafoli, S. Papa), Vol. 671, pp. 244–256.

McConnaughey T. (1989) ^{13}C and ^{18}O isotopic disequilibrium in biological carbonates: II. *In vitro* simulation of kinetic isotope effects. *Geochim. Cosmochim. Acta* **53,** 163–171.

Mehrbach C., Culberson C. H., Hawley J. E., and Pytkowicz R. M. (1973) Measurement of the apparent dissociation constant of carbonic acid in seawater at atmospheric pressure. *Limnol. Oceanogr.* **18,** 897–907.

Millero F. J. and Schreiber D. R. (1982) Use of the ion pairing model to estimate activity coefficients of the ionic components of natural waters. *Am. J. Sci.* **282,** 1508–1540.

Milliman J. D., Troy P. J., Balch W. M., Adams A. K., Li Y.-H., and Mackenzie F. T. (1999) Biologically mediated dissolution of calcium carbonate above the chemical lysocline? *Deep-Sea Res. I* **46,** 1653–1669.

Morse J. W. and Mackenzie F. T. (1990) *Geochemistry of Sedimentary Carbonates, Developments in Sedimentology,* Vol. 48, p. 707. Elsevier.

Morse J. W., Mucci A., and Millero F. J. (1980) The solubility of calcite and aragonite in seawater of 35% salinity at 25°C and atmospheric pressure. *Geochim. Cosmochim. Acta* **44,** 85–94.

Mucci A. (1986) Growth kinetics and composition of magnesian calcite overgrowths precipitated from seawater: Quantitative influence of orthophosphate ions. *Geochim. Cosmochim. Acta* **50,** 2255–2265.

Mucci A. (1987) Influence of temperature on the composition of magnesian calcite overgrowths precipitated from seawater. *Geochim. Cosmochim. Acta* **51,** 1977–1984.

Mucci A. and Morse J. W. (1983) The incorporation of Mg^{2+} and Sr^{2+} into calcite overgrowths: Influences of growth rate and solution composition. *Geochim. Cosmochim. Acta* **47,** 217–233.

Mucci A. and Morse J. W. (1984) The solubility of calcite in seawater solutions at various magnesium concentration, $I_t = 0.697$ m at 25°C and one atmosphere total pressure. *Geochim. Cosmochim. Acta* **48,** 815–822.

Nürnberg D., Bijma J., and Hemleben Ch. (1996) Assessing the reliability of magnesium in foraminiferal calcite as a proxy for water mass temperature. *Geochim. Cosmochim. Acta* **60,** 803–814. Erratum: 2483–2484.

Pörtner H. O., Bock C., and Reipschläger A. (2000) Modulation of the cost of *p*Hi regulation during metabolic depression: A ^{31}P–NMR study in invertabrate (*Sipunculus nudus*) isolated muscle. *J. Exp. Biol.* **203,** 2417–2428.

Preston R. R. (1998) Transmembrane Mg^{2+} currents and intracellular free Mg^{2+} concentration in *paramecium tetraurelia. J. Membrane Biol.* **164,** 11–24.

Rink S., Kühl M., Bijma J., and Spero H. J. (1998) Microsensor studies of photosynthesis and respiration in the symbiotic foraminifer *Orbulina universa. Mar. Biol.* **131,** 583–595.

Sanyal A., Nugent M., Reeder R. R., and Bijma J. (2000). Seawater *p*H control on the boron isotopic composition of calcite: Evidence from inorganic calcite precipitation experiments. *Geochim. Cosmochim. Acta* **64,** 1551–1555.

Simkiss K. (1964) The inhibitory effects of some metabolites on the precipitation of $CaCO_3$ from artificial and natural seawater. *J. Cons. Cons. Perm. Int. Explor. Mer.* **29,** 6–18.

Simkiss K. and Wilbur K. M. (1989) *Biomineralization. Cell Biology and Mineral Deposition,* p. 337. Academic Press.

Sültemeyer D. and Rinast K.-A. (1996) The CO_2 permeability of the plasma membrane of *Chlamydomonas reinhardtii*: mass-spectrometric ^{18}O-exchange measurements from $^{13}C^{18}O_2$ in suspensions of carbonic anhydrase-loaded plasma-membrane vesicles. *Planta* **200,** 358–368.

ter Kuile B. (1991) Mechanisms for calcification and carbon cycling in algal symbiont-bearing foraminifera. In *Biology of Foraminifera* (eds. J. J. Lee and O. R. Anderson), pp. 73–89. Academic Press.

van der Wal P., de Vrind J. P. M., de Vrind-de Jong E. W., and Borman A. H. (1987) Incompleteness of the coccosphere as a possible stimulus for coccolith formation in *Pleurochrysis carterae* (Prymnesiophyceae). *J. Phycol.* **23,** 218–221.

Weiner S. and Erez J. (1984) Organic matrix of the shell of the foraminifer, *Heterostegina depressa. J. Foraminiferal Res.* **14,** 206–212.

Wedborg M., Turner D. R., Anderson L. G., and Dyrssen D. (1999) Determination of *p*H. In *Methods of Seawater Analysis* (eds. K. Grasshoff, K. Kremling, and M. Ehrhardt), pp. 109–125. Wiley-VCH.

Wolf-Gladrow D. A., Bijma J., and Zeebe R. E. (1999) Model simulation of the carbonate system in the microenvironment of symbiont bearing foraminifera. *Mar. Chem.* **64,** 181–198.

Zeebe R. E. (1999) An explanation of the effect of seawater carbonate concentration on foraminiferal oxygen isotopes. *Geochim. Cosmochim. Acta.* **63,** 2001–2007.

Zeebe R. E., Wolf-Gladrow D. A., and Jansen H. (1999) On the time required to establish chemical and isotopic equilibrium in the carbon dioxide system in sea water. *Mar. Chem.* **65,** 135–153.

Zhang Y. and Dawe R. A. (2000) Influence of Mg^{2+} on the kinetics of calcite precipitation and calcite crystal morphology. *Chem. Geol.* **163,** 129–138.

Zuddas P. and Mucci A. (1994) Kinetics of calcite precipitation from seawater: I. A. classical chemical kinetics description for strong electrolyte solutions. *Geochim. Cosmochim. Acta.* **58,** 4353–4362.